Erzincan Üniversitesi
Fen Bilimleri Enstitüsü Dergisi
2023, 16(1), 258-272
ISSN: 1307-9085, e-ISSN: 2149-4584
Araştırma Makalesi

Erzincan University
Journal of Science and Technology
2023, 16(1), 258-272
DOI: 10.18185/erzifbed.1250712
Research Article

Effects of Normal Load and Sliding Distance on the Dry Sliding Wear Characteristics of Invar-36 Superalloy

Yusuf KANCA[1*]

[1]Department of Mechanical Engineering, Faculty of Engineering, Hitit University, 19030, Çorum, Türkiye

Received: 14/02/2023, **Revised:** 23/03/2023, **Accepted:** 23/03/2023, **Published:** 30/03/2023

Abstract

In the present study, the wear and friction behavior of Fe-based Invar-36 superalloy was investigated against an alumina ball under various sliding distances (25, 50, 75 and 100 m) and normal loads (5, 15 and 25 N) using a ball-on-disk tribometer. The worn surfaces were characterized using scanning electron microscopy (SEM) equipped with energy dispersive X-ray spectroscopy (EDS) and 2D-profilometry. The experimental results show that the coefficient of friction (COF) of Invar-36 (0.37-0.51) significantly decreased with increasing normal load, with a minimum value at 25 N. On the other hand, a slight increase in friction coefficient was observed with increasing sliding distance. Moreover, the wear volume of Invar-36 (ranged from 2.63 to 157.17×10^{-3} mm^3) was observed to increase with increasing normal load and sliding distance. The specific wear rate found a constant increase from 1.98-2.99×10^{-5} to 6.33-11.45×10^{-5} mm^3/Nm at increasing normal loads. On the contrary, the wear rate was gradually reduced when the sliding distance was increased especially at higher applied loads, due to the densification process. In addition, the wear mechanism was complex, including oxidation, abrasion, and plastic deformation, became more intense as the normal load or the number of sliding cycles was increased.

Keywords: Invar-36 superalloy, Friction, Wear, Normal load, Sliding distance

Normal Yük ve Kayma Mesafesinin Invar-36 Süper Alaşımının Kuru Kaymalı Aşınma Özellikleri Üzerindeki Etkileri

Öz

Bu çalışmada, demir bazlı Invar-36 süper alaşımın aşınma ve sürtünme davranışı çeşitli kayma mesafeleri (25, 50, 75 ve 100 m) ve yükler (5, 15 ve 25 N) altında alümina top karşıt yüzeyi kullanılarak incelenmiştir. Aşınmış yüzeyler, enerji dağılımlı X-ışını spektroskopisi (EDS) ile donatılmış taramalı elektron mikroskobu (SEM) ve 2D-profilometri kullanılarak karakterize edilmiştir. Deneysel sonuçlar, Invar-36'nın sürtünme katsayısının (0,37-0,51) artan normal yük ile önemli ölçüde azaldığını göstermektedir ve en düşük değer 25 N'da elde edilmiştir. Buna karşın, artan kayma mesafesi ile sürtünme katsayısında çok az bir artış görülmüştür. Ayrıca, yapılan deneylerde 2,63-157,17×10^{-3} mm^3 aralığında bulunan aşınma hacmi değerlerinin artan normal yük ve kayma mesafesi ile yükseldiği gözlenmiştir. Uygulanan yükün artmasıyla aşınma oranı 1,98-2,99×10^{-5}'ten 6,33-11,45×10^{-5} mm^3/Nm'ye çıkmıştır. Aksine, artan kayma mesafesi ile özellikle daha yüksek yükler altında yoğunlaştırma işlemi oluşması nedeniyle aşınma oranı kademeli olarak azalmıştır. Invar-36 yüzeyinde oksidasyon, abrasyon ve plastik deformasyon dahil olmak üzere çok farklı aşınma mekanizmaları oluşmuştur ve bu mekanizmalar artan normal yük veya kayma mesafesi ile daha yoğun hale gelmiştir.

Anahtar Kelimeler: Invar-36 süper alaşım, Sürtünme, Aşınma, Normal yük, Kayma mesafesi

*Corresponding Author: kanca.yusuf@gmail.com
Yusuf Kanca, https://orcid.org/ 0000-0002-8769-0774

1. Introduction

Invar-36 superalloy, as an iron-based iron-nickel alloy, has received wide attention in various applications such as precision measuring instruments, molding tools for aerospace and automotive industries [1-4]. This is because of the material's low coefficient of thermal expansion and high dimensional stability under the Curie temperature as well as its satisfactory chemical resistance [5]. However, the moderate tensile strength and surface hardness [6, 7] restrict the use of Invar-36 in load-bearing articulating applications, owing to its single phase austenite (γ-Fe) crystal structure.

A limited number of studies has been found in literature, investigating the wear and friction behavior of Invar-36. For instance, Kanca (2022) [8] examined the tribological performance of powder-pack borided Invar-36 surfaces in a reciprocating wear apparatus and found that the wear resistance significantly increased after the boriding process and increasing sliding distance caused a higher wear volume. Wang et al. (2023) [9] investigated the cryogenic friction and wear properties of Invar-36 superalloy with temperatures as low as -196 °C under the loads of 0.5-2 N in a rotatory type ball-on-disk tester. The researchers found the reduction in the wear rate and COF of Invar-36 under cryogenic conditions due to self-lubrication effect and lower stress generation on the contact surface. But, there is a lack of research data on Invar-36 alloy under a wide range of loading conditions (from low to high), which should be addressed to explore its tribological performance in more detail and estimate the life of this material under a wide range of loads.

The wear and friction performance of materials has been evaluated using different test parameters such as applied load, sliding distance and sliding speed. The test parameters are defined by considering the service conditions of devices and/or components. That is to say the tribological behavior of materials is significantly affected by the aforementioned test parameters. For instance, increasing applied load generally results is an increase in the wear volume while a decrease in friction coefficients. The lower friction coefficient is associated with the formation of a large number of wear debris and an increase in the surface roughness, which lead to a decrease in contact area between the articulating surfaces.

The present work investigates the tribological performance of Invar-36 alloy against alumina ceramic ball under dry conditions using a ball-on-disk tribometer at room temperature. All tests are carried out at sliding distances of 25, 50, 75 and 100 m and normal loads of 5, 15 and 25 N. This study provides the tribological data (friction coefficient, wear rate and wear mechanism) of Invar 36 alloy against alumina ball under different loads and sliding distances, and provides important experimental guidance for the material's potential to be used in various industries such as automotive and aerospace. The wear mechanisms are determined using a scanning electron microscopy (SEM) equipped with energy dispersive X-ray spectrometer (EDS) map analysis.

2. Materials and Methods

The chemical content of Fe-based Invar-36 superalloy used in the current study is provided in Table 1. Cylindrical samples (nominal diameter 25 mm, thickness 3.5 mm) were subjected to a conventional metallographic preparation process, composed of cold mounting, gradual sanding (320-600-800-1000-1200-2500 SiC) and polishing (1 μm diamond paste).

Table 1. Chemical content (wt.%) of Fe-based Invar-36 superalloy used in the current study.

Material	Fe	Ni	Mn	Si	C
Invar-36	Balance	36.55	0.25	0.16	0.02

The experiments were carried out in dry-sliding conditions on a customized ball-on-disk wear apparatus according to ASTM G-133. The Invar-36 discs were articulated against an alumina ball (diameter 6 mm) at room temperature at the loads of 5, 15 and 25 N and the sliding distances 25, 50, 75 and 100 m. All tests were performed at a stroke length of 5 mm and a sliding velocity of 20 mms^{-1}. The friction coefficient (COF) was calculated as the rate of frictional force (recorded during the wear experiment) to normal load. Mean COF values at the aforementioned sliding distances were calculated by averaging the 6-meter COF data before each specified sliding distance. A list of test parameters is provided in Table 2.

Table 2. Test conditions used for testing in ball-on-disk tribometer.

Test specimens	Upper: alumina ball (Ø6 mm) Lower: Invar-36 disk (Ø25 mm, 3.5 mm)
Stroke length	5 mm
Average sliding speed	20 mm/s
Applied load	5, 15 and 25 N
Sliding distance	25, 50, 75 and 100 m
Test temperature	Ambient

The wear volume (volume loss) was calculated from the wear track profiles obtained using a 2D profilometry (MarSurf M300, Germany), as previously described by Kanca, 2022 [8]. The wear rate (W) was then quantified as follows:

$$W = \Delta V/(FS) \quad \text{(Eq. 1)}$$

Where ΔV: Wear track volume (mm^3), F: Test load (N) and S: Sliding distance (m).

The wear mechanism was examined using a scanning electron microscopy (SEM, Jeol JSM-7001F). Energy dispersive X-ray spectrometer (EDS) map analysis was performed with the same device to investigate the distribution of elements of the wear surfaces.

3. Results and Discussion

3.1. Friction and Wear Behavior

The friction and wear behavior of Invar-36 superalloy was evaluated under dry sliding conditions. Figure 1 demonstrates the coefficient of friction (COF) of Invar-36 superalloy against the alumina ball for the normal loads of 5, 15 and 25 N as a function of sliding distance. The COF of all tests found an initial sharp rise and drop state followed by a steady state. The COF rapidly increased to around 0.5 followed by decreasing to the levels of 0.25-0.33, classified as a running period, as defined in previous studies [10, 11]. Afterwards, the curve showed only a mild increase during the steady state, which can be attributed to the formation of a tribolayer suggested by Kuang et al. (2022) [12]. The steady COFs were found to decrease with increasing normal loads, which were 0.49-0.51, 0.37-0.40, and 0.33-0.35 under the normal loads of 5, 15, and 25 N, respectively.

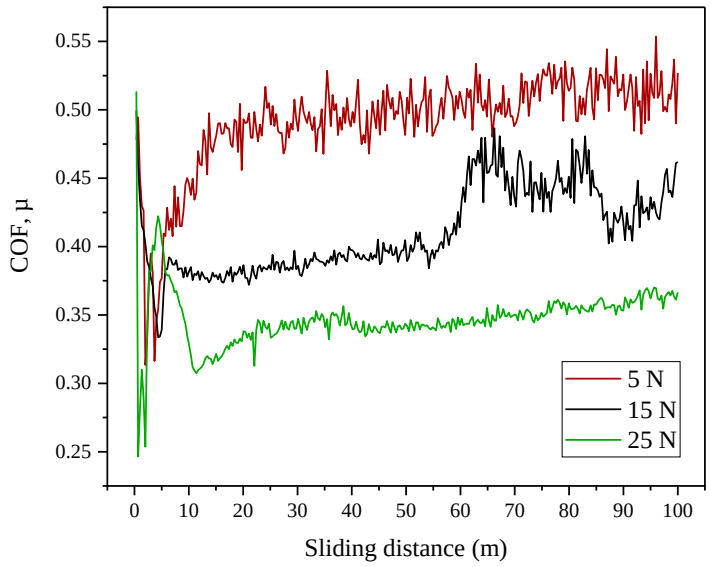

Figure 1. Coefficient of friction (μ) over sliding distance under the loads of 5, 15 and 25 N.

Figure 2 shows the mean COFs obtained from the articulation of Invar-36 surfaces as a function of sliding distance at the loads of 5, 15 and 25 N. The increase in the contact load caused a significant decrease in the COF for any given sliding distance. For instance, at the sliding distance of 25 m, the average friction coefficient was 0.50 under 5 N, which was found to be 0.46 with an 8% decrease as the load increased to 15 N, and 0.41 with a decrease of 18% at 25 N. Similar trend was observed at the sliding distances of 50, 75 and 100 m. Under increased loads there found to be an increase in the contact area between the articulating surfaces (see wear track width and depth values given in Table 3). Even so, it is stated by previous researchers [13, 14] that the increased concentration of wear debris between the two articulating materials at increasing loads leads to a decrease in the real contact area, which might result in the decrease in the COF at higher applied loads in the current work.

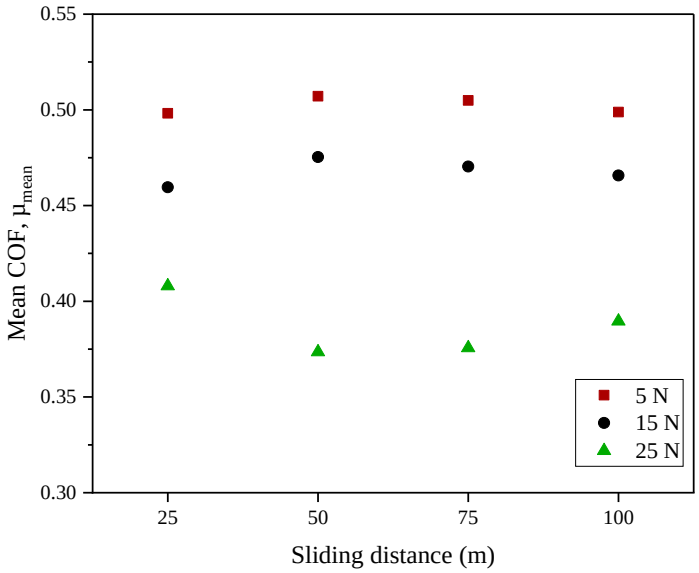

Figure 2. Mean coefficient of friction (μ_m) versus sliding distance at the loads of 5, 15 and 25 N.

After each wear test, 2D wear profiles across the wear tracks were obtained from the Invar-36 surfaces. Figure 3 shows typical wear profiles formed on the Invar-36 surfaces, obtained at the sliding distance of 50 m. The wear track widths and depths were found to increase with increasing normal load and sliding distance (Figure 3 and Table 3). Depending on the applied load and number of sliding cycle, the wear track width and depth values were ranged from 361.3 to 1115.3 μm and from 5.68 to 60.57 μm, respectively. When the normal load increased from 5 to 15 N, the wear track width increased by 98% (at the sliding distance of 25 m), 39% (at 50 m), 36% (at 75 m) and 35% (at 100 m). The increment was found to be 26-44% as the normal load was further increased to 25 N. Under a given normal load from the sliding distance of 25 to 100 m, the wear track width increased by 58% (at 5 N), 8% (at 15 N), and 12% (at 25 N). While, the wear track depth increased by 93% (at 5 N), 60% (at 15 N), and 67% (at 25 N).

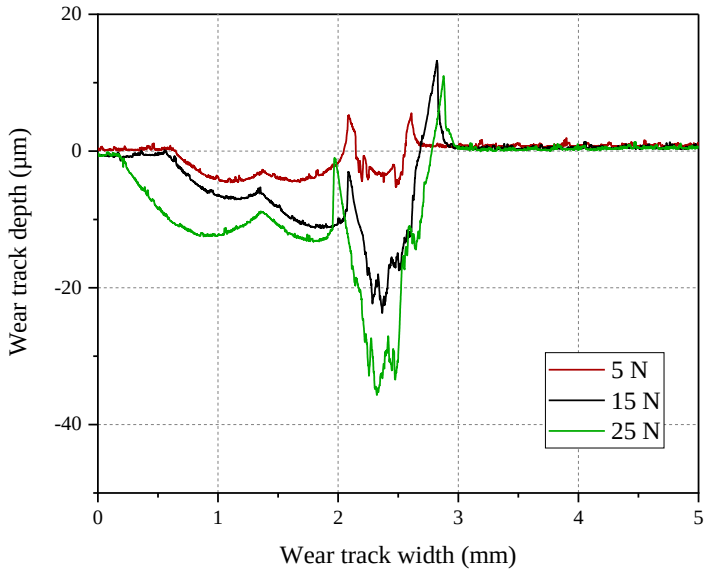

Figure 3. 2D wear track profiles of Invar-36 alloy, subjected to the tests at the sliding distance of 50 m under the loads of 5, 15 and 25 N.

Figures 4 shows the wear volume as a function of the sliding distance under the applied loads of 5, 15 and 25 N. The wear volume increased with the increase in the sliding distance and applied load. For instance, the wear volume increased by 1.5-fold (from 27.53×10^{-3} to 69.25×10^{-3} mm^3) as the sliding distance increased from 25 to 100 m under the applied load of 15 N, and 10.9-fold (from 7.70×10^{-3} to 91.29×10^{-3} mm^3) as the normal load increased from 5 to 25 N under the sliding distance of 50 m. The higher load and reciprocating cycle caused an intensive shear stress and plastic deformation at the articulating asperities and thereby a greater degree of wear volume on the Invar-36 surface. The wear volume was found to be 2.6×10^{-3} mm^3, obtained at the lowest load and distance (5 N and 25 m). While, the most severe wear (157.2×10^{-3} mm^3) happened during the experiment conducted at the maximum applied load and sliding distance (25 N and 100 m). This finding is coincident with the mean surface roughness (R_a) observations (Table 3). The lowest R_a value (0.353 μm) was obtained from the experiment performed at the normal load of 5 N and the sliding distance of 25 m while the highest R_a value (1.953 μm) was obtained from the test conducted at the load of 25 N and the sliding distance of 100 m.

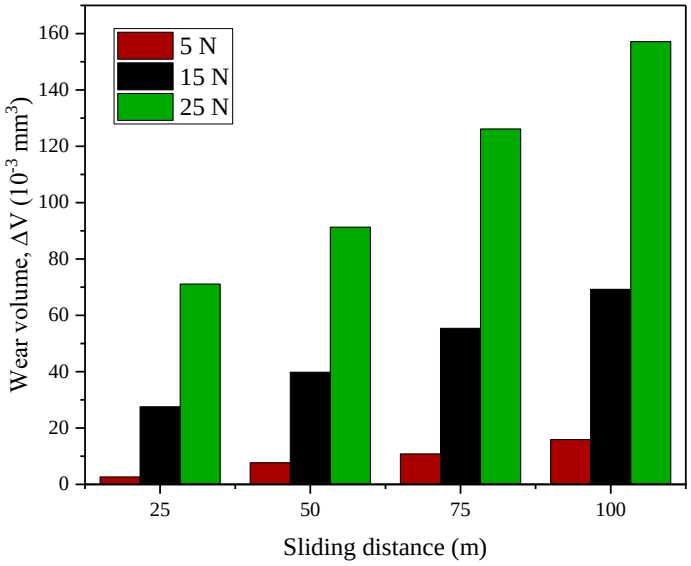

Figure 4. Wear volume of Invar-36 obtained after the articulation against the alumina ball at the loads of 5, 15 and 25 N and the sliding distances of 25, 50, 75 and 100 m.

Figure 5 shows the specific wear rate as a function of the sliding distance, obtained on the Invar-36 surfaces under the applied loads of 5, 15 and 25 N. When the normal load was increased from 5 to 25 N, the specific wear rate was observed to increase constantly from 1.98-2.99×10^{-5} to 6.33-11.45×10^{-5} mm^3/Nm. But, the results were diverse when the number of sliding cycle was increased. At the lowest applied load (5 N), the specific wear rate was increased by 46% (from 1.98×10^{-5} to 2.90×10^{-5} mm^3/Nm) as the sliding distance was increased from 25 to 50 m, and remained around the same level at 75 m (2.72×10^{-5} mm^3/Nm) and 100 m (2.99×10^{-5} mm^3/Nm). At 15 and 25 N, on the other hand, the specific wear rate was reduced with the increase in the sliding distance and the reduction was more remarkable from the sliding distance of 25 to 50 m. The decrease in the wear rate even though the increase in the wear volume indicates a reduction in the wear intensity due to the densification process. The occurrence of wear intensity was reported by Kuang et al. (2022) [12] under elevated normal loads.

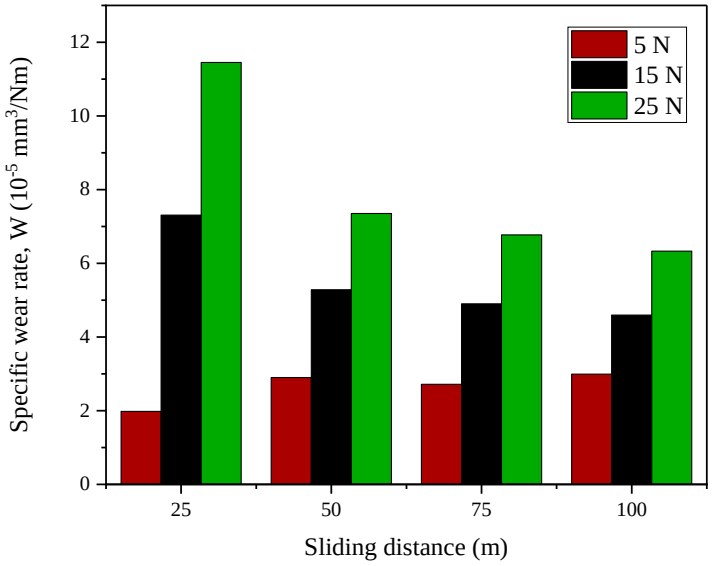

Figure 5. Specific wear rate of Invar-36 at the loads of 5, 15 and 25 N and the sliding distances of 25, 50, 75 and 100 m.

Table 3. Average surface roughness, mean COF, wear track width and depth, volume loss and wear rate of Invar-36 alloy, subjected to dry-sliding reciprocating wear tests under various loads and sliding distances.

Nomenclature	Ra (μm)	Mean COF	Wear track width (μm)	Wear track depth (μm)	Wear volume (10^{-3} mm^3)	Wear rate (10^{-5} mm^3/Nm)
25m-5N	0.353	0.498	361.3	5.68	2.63	1.98
25m-15N	0.924	0.460	716.4	18.84	27.53	7.31
25m-25N	1.753	0.408	993.2	36.25	71.10	11.45
50m-5N	0.562	0.507	526.3	6.79	7.69	2.90
50m-15N	1.066	0.475	729.2	24.47	39.79	5.28
50m-25N	1.285	0.374	936.1	37.42	91.29	7.35
75m-5N	0.681	0.505	568.0	11.78	10.81	2.72
75m-15N	1.037	0.470	774.3	26.69	55.37	4.90
75m-25N	0.830	0.376	975.8	41.97	126.13	6.77
100m-5N	0.669	0.499	571.0	10.97	15.89	2.99
100m-15N	0.756	0.466	772.7	30.05	69.25	4.60
100m-25N	1.953	0.390	1115.3	60.57	157.19	6.33

3.2.Surface Wear Analysis

Photographs, SEM and EDS mapping images of the wear scars obtained from the Invar-36 surfaces undergone a minimum (25m-5N), moderate (100m-5N) and maximum (100m-25N) wear deformation were shown in Figures 6-8. Micro-cracks perpendicular to the sliding direction were seen because of fatigue loading occurred during the wear tests, which indicates the occurrence of plastic deformation on the Invar-36 surface during the articulation. The plastic deformation was more evidence at increased sliding distances and normal loads. Moreover, SEM images obtained from the wear tracks showed micro-scratches parallel to the sliding direction, mainly caused by the plowing of the asperities on the Invar-36 surface. There also found to be the occurrence a large amount of wear debris during the wear test.

The EDS analysis was conducted to detect the oxidation behavior of the wear scars, as shown in Figures 6-8(d-e). There found to be iron (51.1-53.4 wt.%) and nickel (28.3-28.8 wt.%) on the wear tracks, which are available in the chemical composition of Invar-36 (Table 1). The presence of oxygen (17.7-20.2 wt.%) and aluminum (0.2-0.5 wt.%) should be noted, which indicates the oxidation of the surface and a small amount of elemental transfer from the abrasive ball. With the increase in the applied load, there observed to be an increase in oxygen levels due to the effect of increasing temperature and the increased wear of the abrasive ball which triggers the material transfer.

The SEM-EDS investigation on the wear tracks clearly shows that the mechanism of wear failure of Invar-36 alloy was complicated and occurred by the combination of abrasion, plastic deformation, and oxidation, acting simultaneously. The surfaces suffered severe wear when the tests were performed at higher applied loads and sliding distances, as evidenced by deeper and wider wear tracks (Figure 3 and Table 3). The wear track widths of 25m-5N, 100m-5N and 100m-25N were measured as 370.4, 570.3 and 1123.1 μm from the SEM images, respectively (Figures 6-8(b)). These values were consistent with those obtained from 2D profilometry (Figure 3 and Table 3).

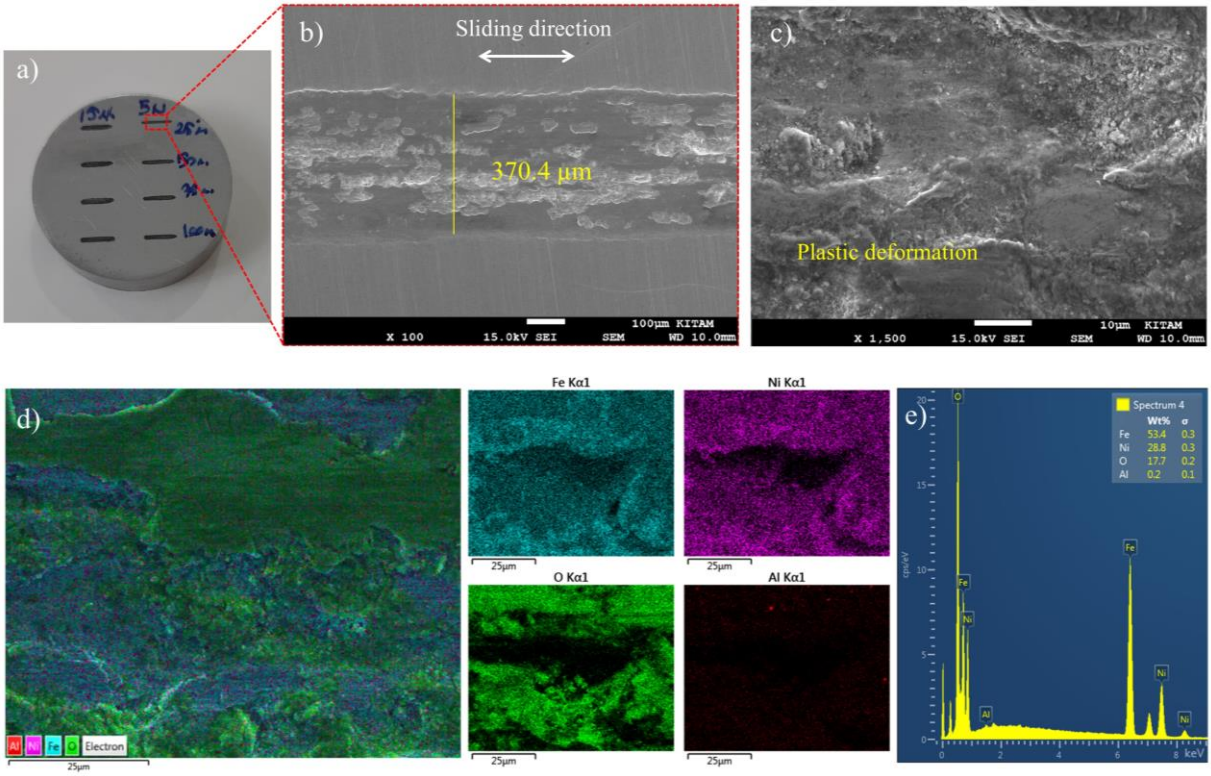

Figure 6. (a) A photograph, SEM images magnified by (b) ×100 and (c) ×1500, (d) EDS mapping and (e) EDS spectra of the worn surface obtained from the experiment performed at the sliding distance of 25 m and the load of 5 N.

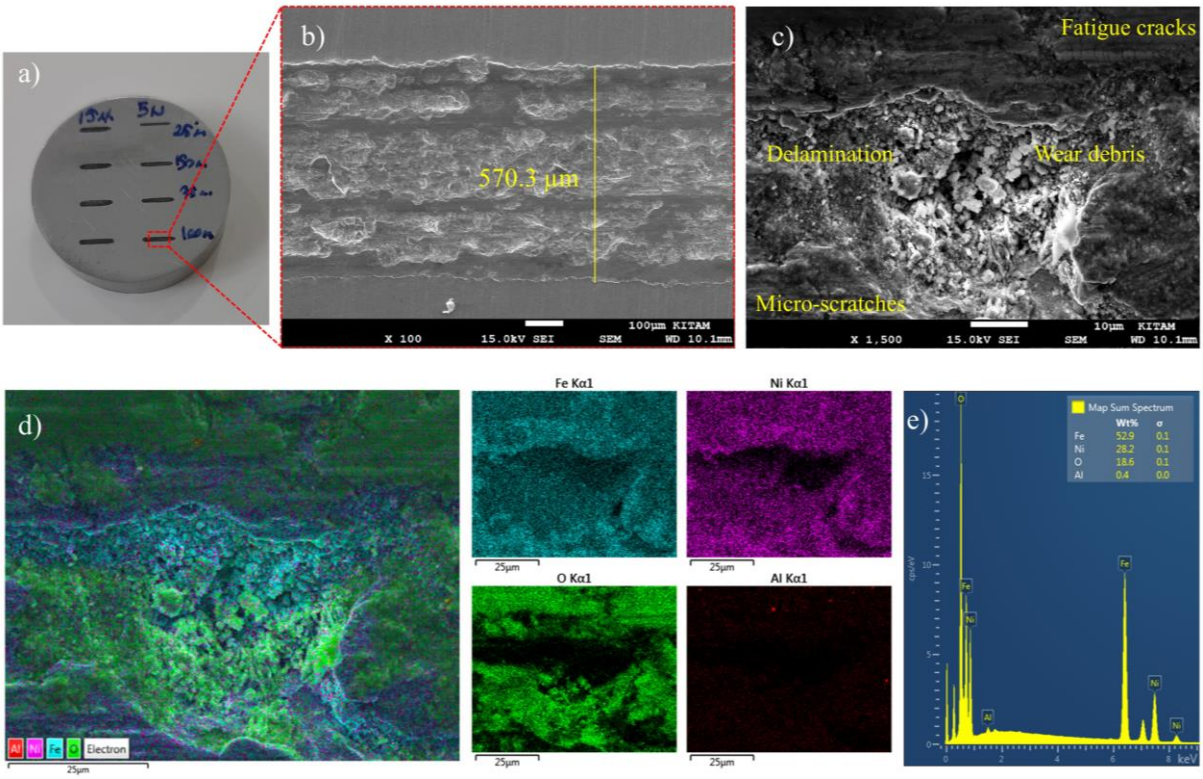

Figure 7. (a) A photograph, SEM images magnified by (b) ×100 and (c) ×1500, (d) EDS mapping and (e) EDS spectra of the worn surface obtained from the experiment performed at the sliding distance of 100 m and the load of 5 N.

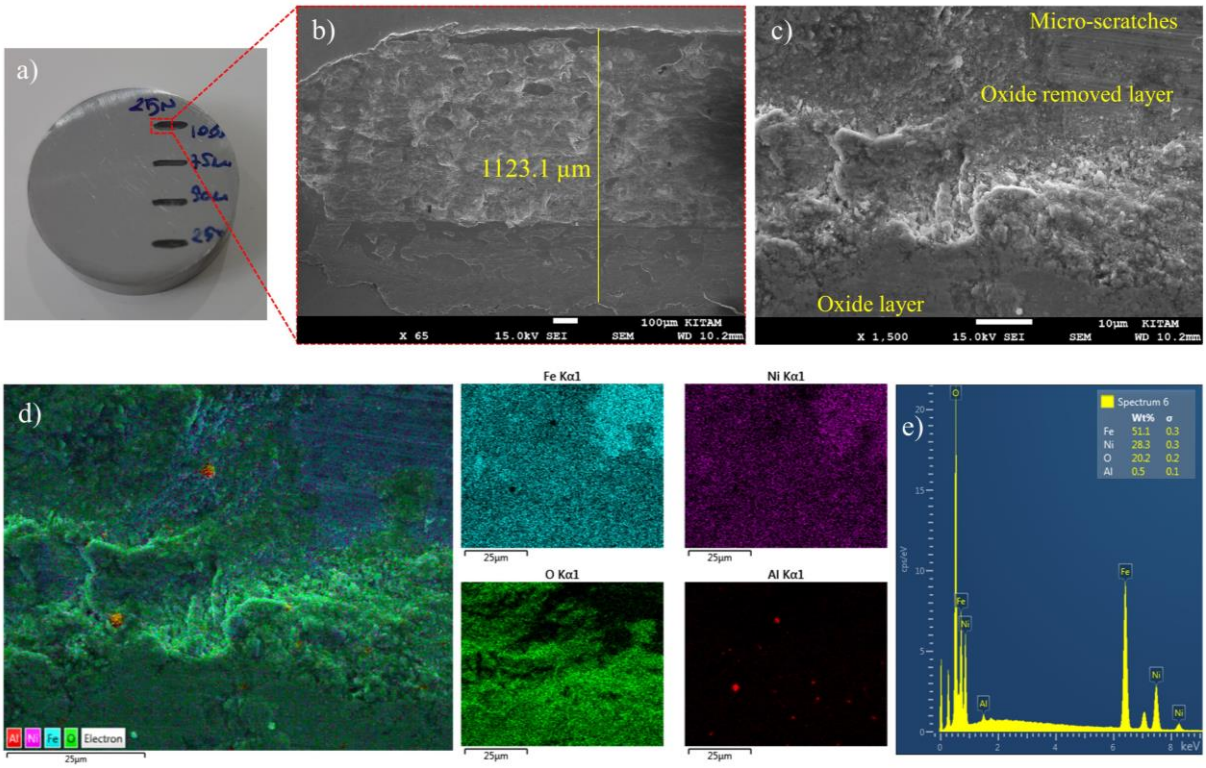

Figure 8. (a) A photograph, SEM images magnified by (b) ×100 and (c) ×1500, (d) EDS mapping and (e) EDS spectra of the worn surface obtained from the experiment performed at the sliding distance of 100 m and the load of 25 N.

4. Conclusions

In the current study, systematic dry sliding wear tests of Fe-based superalloy Invar-36 against alumina ball in a ball-on-disk tribometer using various parameters of sliding distance and normal load was conducted. The following conclusions can be drawn.

1. Both friction coefficient and specific wear rate of Invar-36 are strongly affected by the sliding parameters (the normal load and number of reciprocating cycles).
2. The friction coefficient of Invar-36 (0.37-0.51) was found to decrease with increasing applied load, with a minimum value at 25 N. On the other hand, only a slight increase in the COF was reported with increasing the number of reciprocating cycles.
3. The wear volume of Invar-36 was ranged from 2.63×10^{-3} to 157.17×10^{-3} mm^3. The alloy exhibited higher wear volume at increased applied loads and the number of sliding cycles.
4. A constant increase in the wear rate (from 1.98-2.99×10^{-5} to 6.33-11.45×10^{-5} mm^3/Nm) was observed with the increase in the applied load. But, the wear rate was lowered when the sliding distance was increased especially at higher applied loads, due to the densification process.
5. The wear mechanism on the Invar-36 surfaces was complicated with the combination of oxidation, abrasion, and plastic deformation, which became more intense when the normal load or sliding distance was increased.

Ethics in Publishing

There are no ethical issues regarding the publication of this study.

Author Contributions

YK: Conceptualization, Methodology, Investigation, Resources, Formal analysis, Writing - original draft, Writing - review &editing.

References

[1] Giolli, C., Turbil, M., Rizzi, G., Rosso, M., Scrivani, A., (2009) Wear resistance improvement of small dimension Invar massive molds for CFRP components, Journal of thermal spray technology, 18, 652-664.

[2] Jasthi, B.K., Arbegast, W.J., Howard, S.M., (2009) Thermal expansion coefficient and mechanical properties of friction stir welded Invar (Fe-36%Ni), Journal of materials engineering and performance, 18, 925-934.

[3] Yakout, M., Elbestawi, M.A., Veldhuis, S.C., (2018) A study of thermal expansion coefficients and microstructure during selective laser melting of Invar 36 and stainless steel 316L, Additive manufacturing, 24, 405-418.

[4] Sahoo, A., Medicherla, V.R.R., (2021) Fe-Ni Invar alloys: A review, Materials today: proceedings, 43, 2242-2244

[5] Wu, C., Guo, W., Li, R., Zhao, Y., Zhou, Q., (2020) Thermal effect on oxidation layer evolution and phase transformation in grinding of Fe-Ni super alloy, Materials letters, 275, 128072.

[6] Wei, K., Yang, Q., Ling, B., Yang, X., Xie, H., Qu, Z., et al. (2020) Mechanical properties of Invar 36 alloy additively manufactured by selective laser melting, Materials science and engineering: A, 772, 138799.

[7] Zheng, S., Sokoluk, M., Yao, G., de Rosa, I., Li, X., (2019) Fe–Ni Invar alloy reinforced by WC nanoparticles with high strength and low thermal expansion, SN applied sciences, 1:172.

[8] Kanca, Y., (2022) Microstructural characterization and dry sliding wear behavior of boride layers grown on Invar-36 superalloy, Surface and coatings technology, 449, 128973

[9] Wang, B., Guo, Y., Zhang, Z., Yi, X., Wang, D., (2023) Investigation of cryogenic friction and wear properties of Invar 36 alloy against Si3N4 ceramic balls, Wear, 518-519, 204648

[10] Kanca, Y., Uçgun, M.C., Günen, A., (2022) Microstructural and tribological behavior of pack-borided Ni-based Hastelloy C-276 superalloy, Metallurgical and materials transactions A, 54, 671-687.

[11] Deng, G., Tieu, A.K., Lan, X., Su, L., Wang, L., Zhu, Q., et al., (2020) Effects of normal load and velocity on the dry sliding tribological behaviour of CoCrFeNiMo0.2 high entropy alloy, Tribology international, 144, 106116.

[12] Kuang, W., Qing, M., Wenfeng, D., Yanjun, Z., Biao, Z., Xuebing, W., et al, (2022) Fretting wear behaviour of machined layer of nickel-based superalloy produced by creep-feed profile grinding, Chinese journal of aeronautics, 35, 401-411.

[13] Sarkar, A.D. (1980) Friction and wear. Academic Press.

[14] Panagopoulos, C.N., Giannakopoulos, K.I., Saltas, V., (2003) Wear behavior of nickel superalloy, CMSX-186, Materials letters, 57, 4611-4616.